**Masahiro Kurosaki**
**Tadashi Morioka**
**Kosuke Ebina**
**Masatoshi Maruyama**
**Tomoshige Yasuda**
**Makoto Endoh**

Research and Engineering Division,
Aero-Engine and Space Operations,
Ishikawajima-Harima Heavy Industries Co. Ltd.,
Mizuho-machi, Nishitama-gun,
Tokyo 190-1297, Japan

# Fault Detection and Identification in an IM270 Gas Turbine Using Measurements for Engine Control

*A unique fault detection and identification algorithm using measurements for engine control use is presented. The algorithm detects an engine fault and identifies the associated component, using a gas path analysis technique with a detailed nonlinear engine model. The algorithm is intended to detect steplike changes in component performance rather than gradual change of all components. Component performance deviation (efficiency and flow rate) is represented by a magnitude and a phase. The phase is selected to minimize the error of evaluation matrices. Then the magnitude is computed. By utilizing operational data of the IM270 engine, the compressor and the turbine performance deviation was quantitatively identified.* [DOI: 10.1115/1.1787515]

## 1 Introduction

Recently, research and development of engine performance condition monitoring has become popular. This is motivated not only by economics but also by recent trends in energy conservation and environmental awareness. Currently there are many gas turbines in service without condition monitoring systems. In order to retrofit these engines with monitoring capabilities, it would be convenient to use the existing sensors on the engine. Most late-model gas turbines use an electronic control unit (ECU). Condition monitoring based on the ECU acquired data for engine control may have considerable benefit.

Advanced monitoring systems not only monitor total gas turbine performance deterioration but also identify individual component health. Monitoring component conditions requires pressure and temperature measurements at both the inlet and outlet of the component. Engine speed measurements are also required for rotating components. The ECU does not measure all required parameters. In order to overcome this difficulty, either an engine model or a linear sensitivity matrix relating measurements and performance parameters is needed. However, the number of measurements may not be sufficient to uniquely identify individual component condition. In this paper we propose a unique algorithm using ECU acquired measurements to address this problem. The algorithm can not only detect fault occurrence but also can identify the faulty component with low computational throughput.

Research and development of algorithms to estimate individual component condition was initiated by Urban [1] in the 1970s and followed by Doel [2]. Both programs used a weighted-least-squares approach and were improved to include the capability of identifying a single large-magnitude fault [3]. The development history and approach are well described in Ref. [4]. The weighted-least-squares technique requires a time-consuming optimization iteration when a nonlinear engine model is used in the process. Appropriate weighting factor selection for use in the performance index is crucial and requires significant experience. As a result it is difficult to apply this approach to newly developed engines. Stimulated by recent interest in engine condition monitoring, a variety of methods have been proposed including linear and nonlinear gas path analysis, multioperation point methods, use of neural networks, genetic algorithms, etc. Among them, Aretakis et al. [5] proposed a combinatorial approach to address the problem of having fewer measurements than parameters to be identified. The concept is that the average of the estimations of all of the possible combinations may be close to the actual values of each parameter.

In this study, we propose a unique algorithm that can detect an engine fault and identify the associated component with measurements acquired for engine control use.

The next section introduces the IM270 engine and the nonlinear engine model, which was used with the algorithm. This is followed by a description of the measurements and adjustable parameters. A linear dependency analysis of measurement deviation caused by different components is presented in Section 4. Section 5 describes the proposed fault detection and identification algorithm in detail. A numerical simulation, which quantifies the combined effects of the linear dependency and noise upon the detection and identification capability of the proposed algorithm, is discussed in Section 6. Finally, in Section 7, it is shown that with operational data the algorithm was able to detect an engine fault and quantitatively identify compressor and turbine performance deviations.

## 2 IM270 Engine and Engine Model

The proposed algorithm was developed specifically for the IM270 engine, although the concept is more general and can be applied to many other gas turbine engines. The IM270 with 2-MW output capacity consists of a two-stage centrifugal compressor,

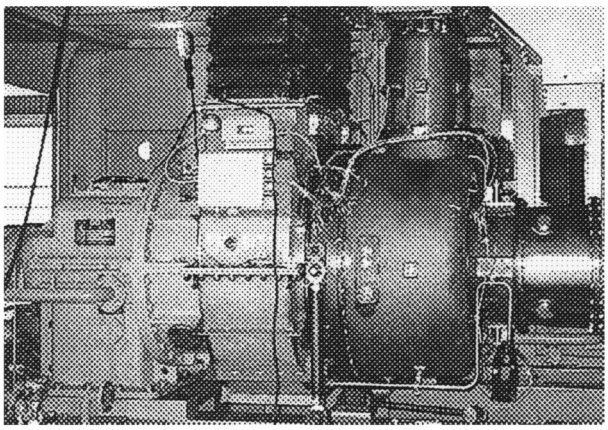

**Fig. 1 IM270 gas turbine**

Contributed by the International Gas Turbine Institute (IGTI) of THE AMERICAN SOCIETY OF MECHANICAL ENGINEERS for publication in the ASME JOURNAL OF ENGINEERING FOR GAS TURBINES AND POWER. Paper presented at the International Gas Turbine and Aeroengine Congress and Exhibition, Atlanta, GA, June 16–19, 2003, Paper No. 2003-GT-38378. Manuscript received by IGTI, October 2002, final revision, March 2003. Associate Editor: H. R. Simmons.

  

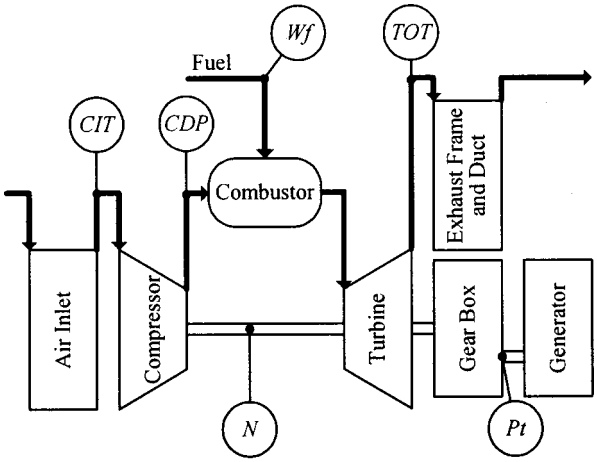


**Fig. 2 Schematic of engine components and sensors**

low $NO_x$ combustor, and a three-stage axial turbine (see Figs. 1 and 2). The features of the IM270 engines are described in Refs. [6,7].

The algorithm is partly based on a nonlinear gas path analysis. A highly accurate engine model is required since several percent of engine component deviation must be identified. The engine model, based on Ref. [8], consists of a compressor, a combustor, and a turbine as shown in Fig. 3. The compressor and turbine characteristics are represented by performance maps. For thermodynamics calculations, specific heat at constant pressure is represented as polynomials, which are functions of temperature and fuel-air ratio. Given engine inlet temperature and pressure, power output, and engine speed, nonlinear equations that represent mass and energy conservation of the gas path as well as a power balance between compressor, generator, and turbine are solved by a Newton-Raphson method. To better match operational data, each performance map was adjusted using correction factors. Figure 4 shows that the measured values and the model output agree very well over a considerable range of power output.

## 3 Fault Detection and Identification

We devised a unique fault detection and identification algorithm for the IM270 engine that can not only detect occurrence of a fault but also can identify the faulty component by using measurements obtained for engine control. This study was motivated by the need to retrofit existing machines with condition monitoring functions without adding sensors.

The engine control unit (ECU) of the IM270 uses the following measurements for engine control: compressor inlet temperature (CIT), compressor discharge pressure (CDP), turbine discharge temperature (TOT), engine speed ($N$), engine power output ($Pt$), and fuel flow ($W_f$), as shown in Fig. 2. Compressor inlet pressure (CIP) is assumed to be equal to the ambient pressure minus a fixed inlet filter pressure loss. These measurements are common to modern gas turbines. Most engine control systems use fuel-air ratio control where CDP is used as a pseudoairflow parameter. It is well known that fuel-air ratio ($W_f$/CDP) has a high correlation with compressor stall margin. In order to ensure stable compressor operation, limiting $W_f$/CDP as a function of corrected speed is a reliable and common method. Moreover, when compressor stall/surge occurs, simultaneous CDP decrease results in a correspond-

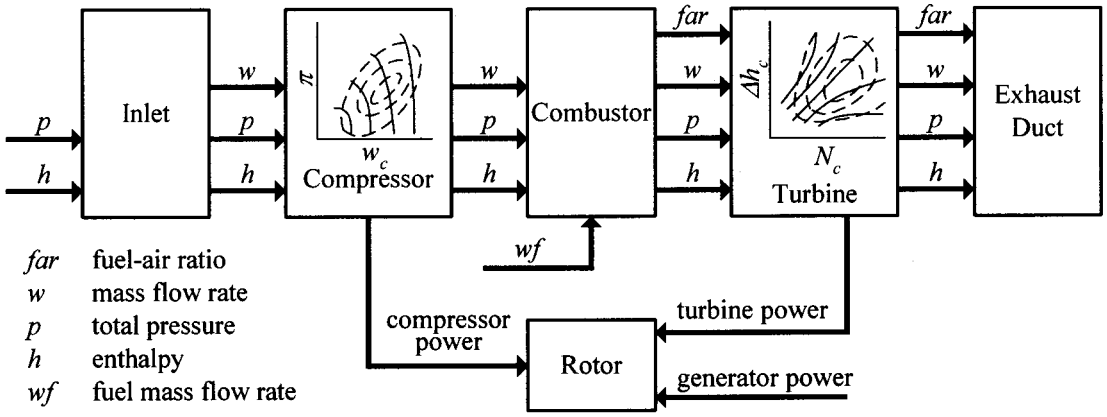


**Fig. 3 Schematic of model components**

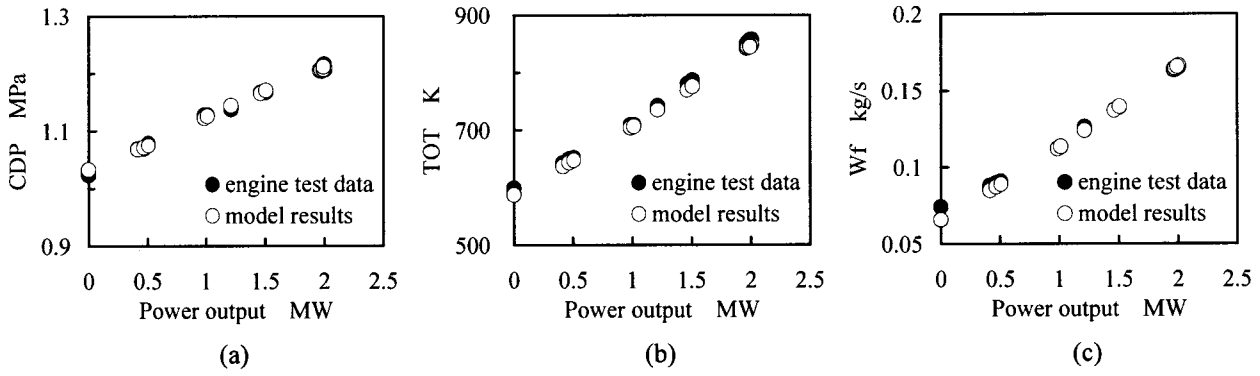


**Fig. 4 Comparison of model results to engine test data: (*a*) compressor discharge pressure; (*b*) turbine outlet temperature; (*c*) fuel mass flow rate**

ing fuel flow decrease preventing further damage. Turbine discharge temperature is clearly an important parameter not only for engine performance but also for engine safety.

The IM270 consists of a compressor, a combustor, and a turbine. The characteristics of the compressor and the turbine are described by corrected mass flow rate and efficiency. These are functions of reduced speed and pressure ratio. Combustor efficiency is also a major performance parameter for gas turbines. Therefore there are at least five parameters to be identified. The correction factors related to those parameters defined below are adjustable:

$$W_{Cc} = Cf_{wc} \times \text{function}_{\text{compressor flow rate}}(N_c, \pi_C)$$

$$\eta_C = Cf_{\eta c} \times \text{function}_{\text{compressor efficiency}}(N_c, \pi_C)$$

$$W_{Tc} = Cf_{wT} \times \text{function}_{\text{turbine flow rate}}(N_c, \pi_T)$$

$$\eta_T = Cf_{\eta T} \times \text{function}_{\text{turbine efficiency}}(N_c, \pi_T)$$

$$\eta_B = Cf_{\eta B} \times \eta_{B\ \text{nominal}}.$$

Given CIT, CIP, $Pt$, and $N$ measurements, the engine model outputs CDP, TOT, and $W_f$. The differences between measured and computed CDP, TOT, and $W_f$ are used to estimate component performance deviation. It is possible to eliminate the differences by adjusting the correction factors. However, by adjusting the five correction factors with only three measurements available, there are an infinite number of solutions. This situation is common for most of gas turbine engine condition monitoring tasks: namely, there are more adjustable parameters than available measurements, making algorithm development challenging.

In order to overcome this difficulty, throughout this study single component fault is assumed since simultaneous multiple faults are unlikely to occur. This assumption reduces the number of unknown parameters from 5 to at most 2.

## 4 Ability to Identify and Linear Dependency

When different combinations of parameter deviations cause identical measurement deviation, it is impossible to identify them separately. It is important to know a priori that the sensor system can identify the type of fault. The ability to identify any two faults can be determined by examining the linear dependency of the measurement deviation vectors caused by the parameter deviations. When the measurement deviation vectors are linearly dependent, it is impossible to distinguish them from each other. Taking the inner product checks the linear dependency of the vectors. When the inner product of the normalized vectors is 1, the two vectors are linearly dependent.

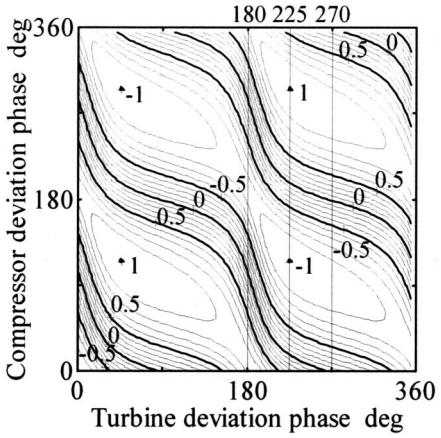


**Fig. 5 Linear dependency of compressor fault and turbine fault**

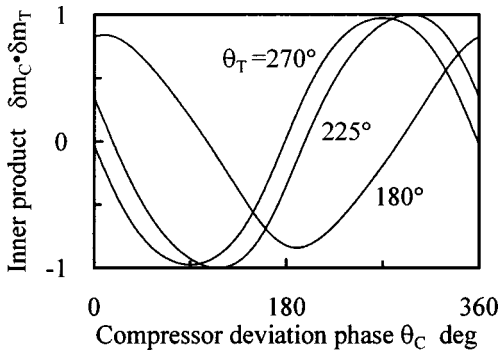


**Fig. 6 Linear dependency of compressor fault for fixed turbine faults**

When the parameter deviations are small, the relation between measurements and parameters are linear and written as follows:

$$\delta m = S \cdot \delta P, \tag{1a}$$

$$\delta m = \begin{pmatrix} \delta\text{CDP} \\ \delta\text{TOT} \\ \delta W_f \end{pmatrix}, \quad \delta P = \begin{pmatrix} \delta\eta_C \\ \delta W_C \\ \delta\eta_T \\ \delta W_T \\ \delta\eta_B \end{pmatrix}.$$

$S$ is the sensitivity matrix and $\delta$ is the normalized deviation from the nominal value. The sensitivity matrix computed by the engine model at the design point with 2-MW output is shown below. Each parameter was changed by $\pm 1\%$ and 2%. The relations were reasonably linear,

$$S = \begin{pmatrix} -0.2796 & 0.7056 & -0.3969 & -0.7509 & -0.0059 \\ -0.5801 & -0.3827 & -0.8492 & 0.1188 & 0.0409 \\ -0.7286 & 0.0047 & -1.7379 & 0.4177 & -1.0055 \end{pmatrix}. \tag{1b}$$

In order to determine the ability to identify compressor and turbine faults with existing sensors, the normalized efficiency and flow rate deviation of them is represented by a magnitude and a phase as follows. Since the deviation magnitude does not affect the linear dependency check, the magnitude is set to unity,

$$\left.\begin{aligned} \delta\eta_C &= \sin\theta_C \\ \delta W_C &= \cos\theta_C \\ \delta P_C &= (\delta\eta_C \quad \delta W_C \quad 0 \quad 0 \quad 0)^T \end{aligned}\right\}, \tag{2}$$

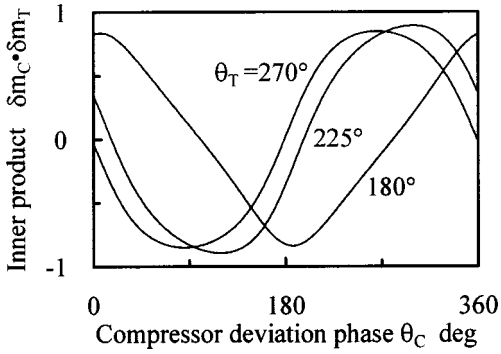


**Fig. 7 Linear dependency of compressor fault with compressor discharge temperature**

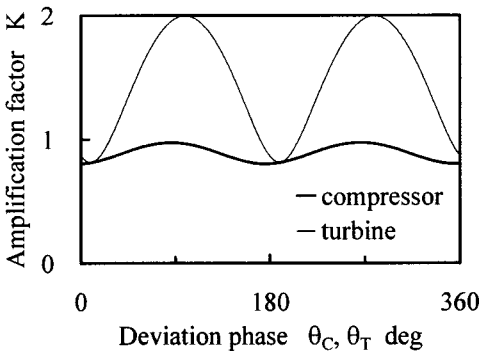


**Fig. 8 Magnitude of measurement deviation due to compressor and turbine fault**

$$\left.\begin{aligned}\delta\eta_T &= \sin\theta_T \\ \delta W_T &= \cos\theta_T \\ \delta P_T &= (0 \;\; 0 \;\; \delta\eta_T \;\; \delta W_T \;\; 0)^T\end{aligned}\right\}. \tag{3}$$

$\delta P_C$ and $\delta P_T$ are the parameter deviation vectors of the compressor and turbine, respectively.

By taking $\theta_C$ and $\theta_T$ from 0 to $2\pi$, all combinations of compressor and turbine performance deviations can be examined. The measurement deviation vectors resulting from compressor and turbine deviations are expressed as follows:

$$\left.\begin{aligned}\delta m_C &= S\cdot\delta P_C \\ \delta m_T &= S\cdot\delta P_T\end{aligned}\right\}. \tag{4}$$

The linear dependency of the $\delta m_C$ and $\delta m_T$ provides information about the ability to identify compressor and turbine faults with the existing measurement system.

Figure 5 shows the linear dependency of the compressor and turbine performance deviations. There are regions where the inner product becomes nearly 1. Since it is impossible to distinguish compressor fault or turbine fault in these regions, other means such as physical reasoning are required. Figure 6 shows that the linear dependency varies with compressor deviation phase $\theta_C$ along the constant turbine deviation phase lines shown in Fig. 5. It is possible to theoretically distinguish between compressor and turbine fault when the inner product is not 1. However, there exists measurement noise that may degrade the quality of the signals. Noise effects on detection capability are discussed in a later section.

Figure 7 shows that when the compressor discharge temperature is known, regions of inner product equal to 1 are eliminated. This is a desirable condition for diagnostics since it is possible to determine the type of fault throughout the entire region; namely, all combinations of efficiency and flow rate deviation are distinguishable. In this paper, however, the capability of the fault detection and identification of the sensor system without the compressor discharge temperature measurement is explored.

Compressor and turbine faults are not linearly dependent with any combustor efficiency fault. Combustor flow rate faults and combustor pressure loss deviations were not studied in this paper.

Thus far, we have discussed the phase of the component performance deviation vector. In order to study fault detection ability, it is necessary to know the amplitude relations among performance and measurement deviation vectors and noise vectors. The amplification factor $K$ is defined as follows:

$$|\delta m| = K|\delta P|, \tag{5}$$

where $|\delta m|$ and $|\delta P|$ are the magnitude of the measurement and parameter deviation vectors. As shown in Fig. 8, the amplification factor $K$ of the compressor is nearly constant regardless of the value of the phase. On the other hand, $K$ of the turbine varies with the phase. For turbine efficiency and flow capacity, $K$ is about 2 and 1, respectively.

When the noise vector $\delta n$ is perpendicular to the measurement deviation vector, the noise effect on the solution error is the largest. The inner product of the noise contaminated measurement deviation vector $\delta m+\delta n$ and the measurement deviation vector $\delta m$ is approximately $1-\frac{1}{2}(|\delta n|/|\delta m|)^2$ when $|\delta n|/|\delta m| \ll 1$. For 20% of noise level-to-measurement deviation, the inner product is approximately 0.98.

## 5 Fault Detection and Identification Algorithm

If two adjustable parameters are fixed to their respective nominal values, the number of equations and unknown parameters are the same. Therefore three adjustable parameters are computed by nonlinear equation solving techniques such as the Newton-Raphson method. All ten possible combinations were computed. Four of them were found to be numerically unstable while the following six cases were stable (see Table 1).

Suppose that a compressor related fault occurs. The measurements may differ from the nominal values as follows:

$$\begin{pmatrix}\delta\text{CDP}\\ \delta\text{TOT}\\ \delta W_f\end{pmatrix} = \begin{pmatrix}s_{11} & s_{12}\\ s_{21} & s_{22}\\ s_{31} & s_{32}\end{pmatrix}\begin{pmatrix}\delta\eta_C\\ \delta W_C\end{pmatrix}. \tag{6}$$

In the case where $\eta_C$ and $W_C$ are fixed, the adjustable parameters are computed by

$$\begin{pmatrix}\delta\eta_T^*\\ \delta W_T^*\\ \delta\eta_B^*\end{pmatrix} = \begin{pmatrix}s_{13} & s_{14} & s_{15}\\ s_{23} & s_{24} & s_{25}\\ s_{33} & s_{34} & s_{35}\end{pmatrix}^{-1}\begin{pmatrix}s_{11} & s_{12}\\ s_{21} & s_{22}\\ s_{31} & s_{32}\end{pmatrix}\begin{pmatrix}\delta\eta_C\\ \delta W_C\end{pmatrix}. \tag{7}$$

From possible combinations, the following matrix is obtained. Each column vector consists of the corresponding adjustable parameters of each case:

$$M = ((\delta P_1^*),(\delta P_2^*),(\delta P_3^*),(\delta P_4^*),(\delta P_5^*),(\delta P_6^*)), \tag{8}$$

where $\delta P_4^* = (0\;0\;\delta\eta_T^*\;\delta W_T^*\;\delta\eta_B^*)^T$, etc. These vectors are called pseudoparameter deviation vectors in order to distinguish them from the real parameter deviation vectors. The matrix is called a pseudoparameter deviation matrix.

When the engine performance deviates from the nominal values, the measurement values also deviate. Given the measurement deviation vectors, the engine model can compute the pseudoparameter deviation vectors $\delta P_{E\,i}^*$ and the pseudomatrix $M_E$. The average magnitude of the pseudoparameter deviation vectors can be used for fault detection purposes,

$$\zeta = \frac{1}{6}\sum_{i=1}^{6}|\delta P_{E\;i}^*|. \tag{9}$$

$|\delta P_{E\,i}^*|$ is the magnitude of $i$th pseudoparameter deviation vector.

The next step is to identify the faulty component. First, the compressor fault is assumed to be

**Table 1 Numerically stable combinations of adjustable parameters**

| | $\eta_C$ | $W_C$ | $\eta_T$ | $W_T$ | $\eta_B$ |
|---|---|---|---|---|---|
| Case 1 | compute | compute | fix | compute | fix |
| Case 2 | compute | compute | fix | fix | compute |
| Case 3 | fix | compute | compute | compute | fix |
| Case 4 | fix | fix | compute | compute | compute |
| Case 5 | compute | fix | fix | compute | compute |
| Case 6 | fix | compute | compute | fix | compute |

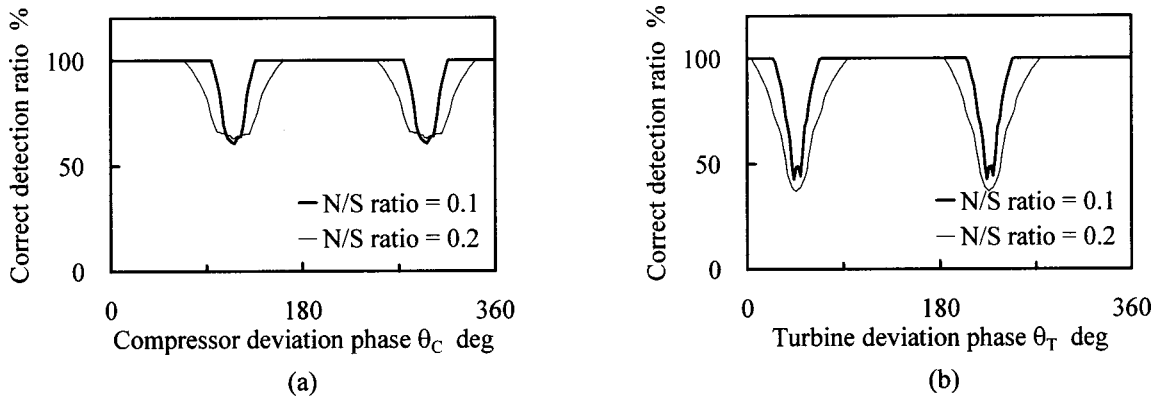


**Fig. 9 Correct identification ratio: (*a*) ratio for compressor fault; (*b*) ratio for turbine fault**

$$\left.\begin{aligned}\delta\eta_C &= R_C \sin\theta_C \\ \delta W_C &= R_C \cos\theta_C\end{aligned}\right\}. \tag{10}$$

Using the sensitivity matrix, the pseudoparameter deviation vectors $\delta P^*_{C\,i}$ and the pseudomatrix $M_C$ are computed. Setting $R_C = 1$, the matrix $M_C$ becomes a function of $\theta_C$,

$$M_C = fn(\theta_C). \tag{11}$$

After normalizing each column vector of the matrix $M_C$ and $M_E$, $\theta_{C\,\mathrm{fit}}$, which gives minimum error, is selected as the phase of the compressor fault and $(\delta P^*_{C\,\mathrm{fit}})_i$ is computed. $R_C$ is computed as the ratio of the magnitudes of the column vectors,

$$R_C = \frac{1}{6}\sum_{i=1}^{6}\frac{|\delta P^*_{E\,i}|}{|(\delta P^*_{C\,\mathrm{fit}})_i|}. \tag{12}$$

Finally, the residual error is computed from the following:

$$\left.\begin{aligned}E_{C\,\mathrm{abs}} &= \sqrt{\frac{1}{6}\sum_{i=1}^{6}|\delta P^*_{E\,i} - (\delta P^*_{C\,\mathrm{fit}})_i|^2} \\ E_{C\,\mathrm{rel}} &= \frac{E_{C\,\mathrm{abs}}}{R_C}\end{aligned}\right\}. \tag{13}$$

Similarly, $\theta_T$, $R_T$, and $E_T$ for the turbine are computed. The faulty component is the one that gives smaller residual error.

The above-mentioned procedure is summarized as follows:

(a) Compute the pseudoparameter deviation vector $\delta P^*_{E\,i}$ and matrix $M_E$ by using the detailed nonlinear engine model with measurements (Eq. (8)).

(b) Detect a fault by using the average magnitude of the pseudoparameter deviation vectors $\zeta$ (Eq. (9)).

(c) Assume a compressor fault as Eq. (10).

(d) Compute $\delta P^*_{C\,i}$ and $M_C$ as a function of phase by using the sensitivity matrix $S$ (Eq. (11)).

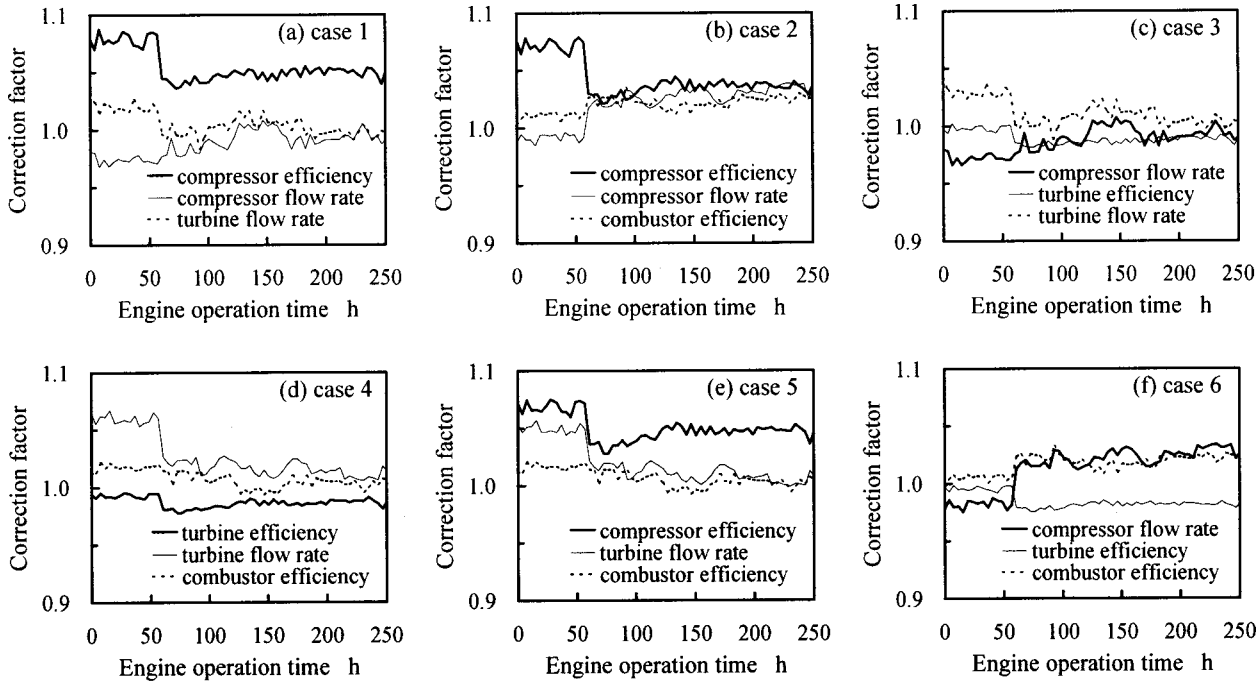


**Fig. 10 Time history of correction factor deviation**

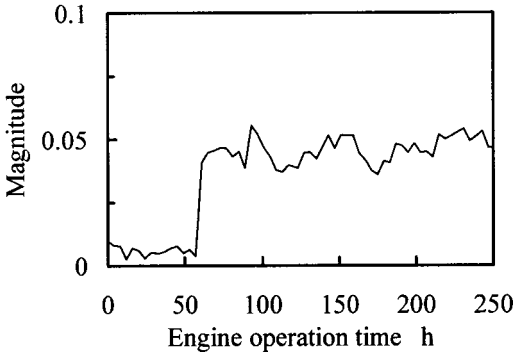


**Fig. 11 Time history of average magnitude of pseudoparameter deviation vectors**

(e) Find the phase $\theta_{C\,\mathrm{fit}}$ which gives minimum error of the normalized $\delta P^*_{E\,i}$ and $\delta P^*_{C\,i}$.

(f) Compute the magnitude $R_C$ and the residual error $E_C$ as Eqs. (12) and (13), respectively.

(g) Repeat the procedure from (c) through (f) for the turbine.

(h) Identify the faulty component by comparing the residual errors $E_C$ and $E_T$.

## 6 Numerical Simulation

In order to evaluate the combined effects of linear dependency and noise on the correct identification ratio, a numerical simulation was conducted. As shown in Fig. 9 the correct identification ratio varies with the phase of the fault. At phases where the linear dependency is nearly unity the correct identification ratio falls to 50% as expected. The ratio also decreases as the noise magnitude level increases. The thick line and the thin line show 0.1 and 0.2 noise levels over parameter deviation ratio, respectively.

## 7 Application to Operational Data

The algorithm was applied to the actual IM270 operational data that were acquired by the ECU. Figure 10 shows the time history of the correction factor deviations computed by the engine model with the measurements.

Figure 11 shows the average magnitude of these pseudoparameter deviation vectors. A significant jump in magnitude from about 1% to 5% at time 61 h can be clearly seen. Figures 12(*a*) and (*b*) show the time history of the phase and magnitude of the compressor performance deviations, respectively. The fluctuating phase converges to a nearly constant 300 deg after the event. The magnitude jumps from nearly 1% to 4% and remains at that level after the event. The phase and magnitude correspond to −3.5% and +2% efficiency and flow rate deviations, respectively. Figure 12(*c*) shows a polar graph of the compressor performance deviation.

Figure 13 shows the turbine performance deviation. Similar observations are obtained. For the turbine, the magnitude and the phase were found to be 5% and 200 deg, respectively, which correspond to −1.7% and −4.7% efficiency and flow rate deviation, respectively.

Figure 14 shows the average relative and absolute error magnitude of the pseudoparameter deviation vectors for the compressor and the turbine, respectively. Both figures indicate that after the

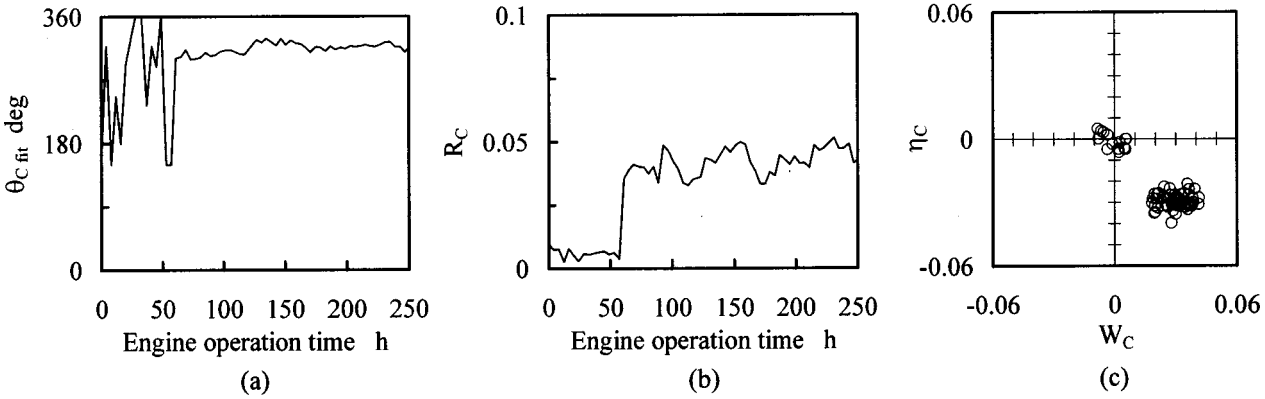


**Fig. 12 Compressor fault detection: (*a*) time history of compressor fault phase; (*b*) time history of compressor fault magnitude; (*c*) polar diagram of compressor fault**

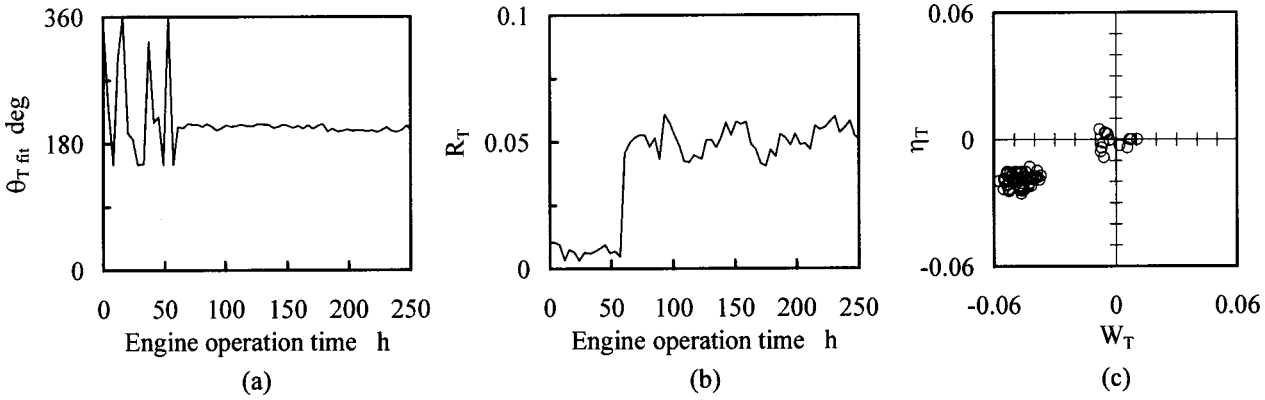


**Fig. 13 Turbine fault detection: (*a*) time history of turbine fault phase; (*b*) time history of turbine fault magnitude; (*c*) polar diagram of turbine fault**

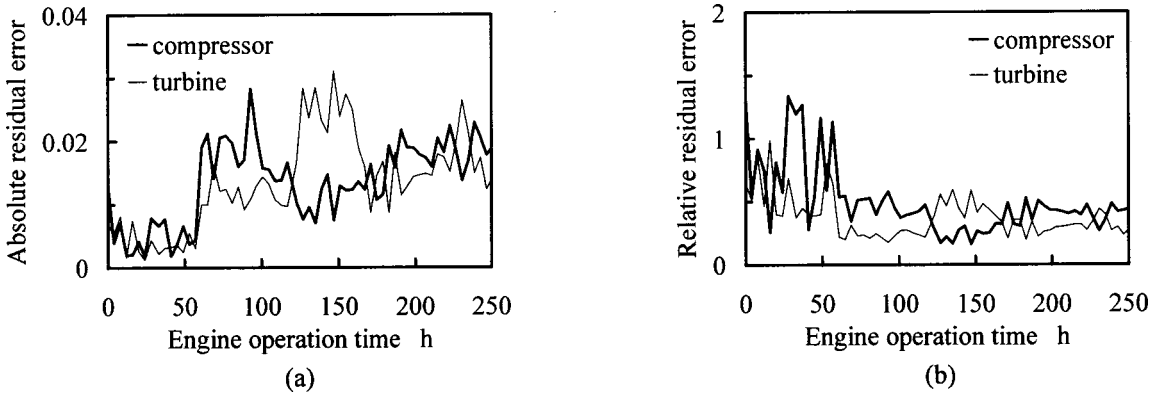


**Fig. 14 Time history of identification error: (*a*) absolute identification error; (*b*) relative identification error**

event, at time 61–123 h, the turbine error magnitude is smaller than that of the compressor. On the contrary, from time 123–191 h the turbine errors are greater than those of the compressor. The turbine error magnitude is again smaller after time 191 h. It is difficult to determine which component is responsible. This ambiguity stems from the linear dependency of the measurement deviation vectors (see Fig. 6). Turbine malfunction was found to be responsible for the event after the engine was disassembled and inspected.

## 8 Conclusions

The proposed fault detection and identification algorithm has the following features:

(i) Only measurements acquired for the engine control are used. No additional measurements are required.

(ii) The number of available measurements may be smaller than parameters to be identified.

(iii) Weighting factors that require significant experience are not necessary. It is easily applied to newly developed engines.

(iv) An accurate engine model and a sensitivity matrix about the operating point are required for correct fault detection and identification.

Given IM270 operational data, the algorithm was able to quantitatively identify the efficiency and the flow rate deviation of the compressor and the turbine, assuming a single component fault.

There remains some ambiguity regarding which component is responsible for the sudden performance deviation. It was shown that this was due to the high linear dependency of the measurement deviation vectors. Addition of a compressor discharge temperature sensor would improve detection and identification.

In this study only the efficiency deviation was considered for the combustor. It is straightforward to extend the algorithm to include the combustor flow rate or pressure loss deviation.

## Acknowledgment

This study was funded by an in-house research fund.

## Nomenclature

CDP = compressor discharge pressure
$Cf_{WC}$ = compressor mass flow rate correction factor
$Cf_{WT}$ = turbine mass flow rate correction factor
$Cf_{\eta B}$ = combustor efficiency correction factor
$Cf_{\eta C}$ = compressor efficiency correction factor
$Cf_{\eta T}$ = turbine efficiency correction factor
CIT = compressor inlet temperature
$E$ = residual error magnitude of pseudoparameter deviation matrix
$M$ = pseudoparameter deviation matrix
$m$ = measurement vector
$N$ = engine rotor speed
$N_c$ = corrected engine rotor speed
$P$ = parameter vector
$R$ = magnitude of component fault
$S$ = sensitivity matrix
TOT = turbine outlet temperature
$W_C$ = compressor mass flow rate
$W_{Cc}$ = corrected compressor mass flow rate
$W_f$ = fuel mass flow rate
$W_T$ = turbine mass flow rate
$W_{Tc}$ = corrected turbine mass flow rate
$\delta P^*$ = pseudoparameter deviation vector
$\delta x$ = normalized deviation from nominal value $(=x-x_{\text{nominal}}/x_{\text{nominal}})$
$\eta_B$ = combustor efficiency
$\eta_C$ = compressor efficiency
$\eta_T$ = turbine efficiency
$\pi_C$ = compressor pressure ratio
$\pi_T$ = turbine pressure ratio
$\theta$ = phase of component fault
$\zeta$ = average magnitude of pseudoparameter deviation vector

### Sub- and Superscripts

$C$ = compressor
$E$ = engine model derived
$T$ = turbine
$*$ = pseudoparameter vector or its element

## References

[1] Urban, L. A., 1972, "Gas Path Analysis Applied to Turbine Engine Condition Monitoring," AIAA/SAE Paper 72–1082.
[2] Doel, D. L., 1994, "TEMPER—A Gas Path Analysis Tool for Commercial Jet Engines," ASME J. Eng. Gas Turbines Power, **116**, pp. 82–89.
[3] Volponi, A. J., 1982, "A Large Measurement Error Recovery Algorithm for Gas Turbine Module Performance Analysis," Hamilton Standard Report No. 3430.
[4] Doel, D. L., 2002, "Interpretation of Weighted-Least-Squares Gas Path Analysis Results," ASME Paper GT-2002-30025.
[5] Aretakis, N., Mathioudakis, K., and Stamatis, A., 2002, "Non-Linear Engine Component Fault Diagnosis From a Limited Number of Measurements Using a Combinatorial Approach," ASME Paper GT-2002-30031.
[6] Kobayashi, H., Tugumi, S., Yonezawa, Y., and Imamura, R., 1996, "2MW Class High Efficiency Gas Turbine IM270 for Co-Generation Plants," ASME Paper 96-GT-001.
[7] Yonezawa, Y., Imamura, R., and Kobayashi, H., 1998, "Development of 2MW Class Gas Turbine IM270 for Co-Generation Plants," Proc. 22th CIMAC.
[8] Sellers, J. F., and Daniele, C. J., 1975, "DYNGEN—A Program for Calculating Steady-State and Transient Performance of Turbojet and Turbofan Engines," NASA TN D-7901.